

МОНІТОРИНГ, ДІАГНОСТИКА ТА КЕРУВАННЯ ЕНЕРГЕТИЧНИМИ ПРОЦЕСАМИ ТА ОБЛАДНАННЯМ MONITORING, DIAGNOSTICS AND MANAGEMENT OF ENERGY PROCESSES AND EQUIPMENT

M. Abdulhamid
AL-Hikma University, Iraq
O. Billy
University of Nairobi, Kenya

STUDY OF DISTRIBUTED SLACK BUS MODEL FOR ECONOMIC DISPATCH OF RENEWABLE ENERGY

Abstract: In this paper, a distributed slack bus (DSB) using combined participation factors based on scheduled generation capacities of the system is designed in order to distribute the system losses among the generators. A DSB algorithm is developed and implemented using a Newton Raphson (NR) solver on a MATLAB platform. The IEEE 14 bus is used as a case study. Renewable energy (RE) sources are introduced into the system and the generation cost compared between systems with renewable energy sources and those with only thermal generators in both the single slack bus (SSB) model and the DSB model. The DSB employed resulted in a reduction in overall real power generation from 272.593 MW to 272.409 MW in the 14 bus model and cost of generation also decreased in both buses. Real power line losses also reduced in the buses. The change in the generation levels of the voltage controlled buses resulted in a proper economic dispatch scheme which gave an accurate representation of the network parameters. The cost of generation is considerably reduced upon introduction of wind and solar generators into the system as compared to systems without these sources. An even more accurate network model is obtained by using combined participation factors.

Keywords: Distributed slack bus; renewable energy

1. Introduction

Economic dispatch is the process of ensuring that the total load is appropriately shared the generating units operating in parallel in a power system. It uses two notions as its basis, the first is that the generating units must provide for the load requirements of the power system within the minimum cost bracket by optimally using the units. The second is that the generating units must be able to provide back up if other units fail. However, this is constrained within a margin [1].

The slack bus is the bus that provides additional real and reactive power to supply the transmission losses in a power system. It is also taken as the reference where the magnitude and phase angle are taken. It is the reference bus for voltage measurements [1].

The use of a distributed slack bus is a technique of removing the concentrated burden of the slack bus by distributing losses to each generator bus in the power system. This results in the system generators adjusting their outputs appropriately subject to their operational limits in order to achieve economic operation. The model was designed to remedy the inadequacies of the single slack bus model which does not exist in actual power systems. This has been motivated by the increase in distributed generation, deregulation and liberalization of the power generation sector [1].

Renewable energy is energy that utilizes sources that are continually replenished by nature to produce usable forms of energy. Examples of these sources include, the sun, wind, water, the earth's heat and plants. This study is interested in two types of renewable energy: wind and solar.

Wind energy is really just another form of solar energy. Sunlight falling on oceans and continents causes air to warm and rise, which in turn generates surface winds. The wind has been used by humans for thousands of years, first to carry ships across oceans and, later, to pump water and grind grain. More recently, wind has been harnessed as a clean, safe source of electricity [1].

Solar energy being in abundance almost all over the country is justifiably seen as the ultimate resource to tap. Although mainly supplemental in nature, it also addresses the problems of atmospheric pollution and climate change [1].

2. Design methodology

2.1 Formation of the improved Newton Raphson matrix

The DSB model selected involves the implementation of a participation factor based on real power generation at generator buses. The selected participation factor implemented using a NR solver results in a change in the conventional NR matrix [2]. The changes made include designating the slack bus as a generator bus and including it in the Jacobian and introducing a participation factor in the Jacobian matrix [3]. This results in the formation of a matrix known as the extended Jacobian (J_e). The Jacobian matrix loses its symmetry and its new size is given by: $(2n-m) \times (2n-m-1)$. Where n is the total number of buses in the system and m represents the number of generator buses. A real power loss term (P_{Loss}) which is multiplied by the participation factors in also included in the corrections matrix. The total real power (P_i) injection in the system thus changes and is given by:

$$P_i = \sum_{k=1}^n |V_i| |V_k| |Y_{ik}| \cos(\theta_{ik} + \delta_k - \delta_i) + K_i(i) * P_{Loss} \tag{1}$$

Where V_i is the voltage at the i th bus, V_k is the voltage at the k th bus, Y_i is the admittance, δ is the voltage angle, and K_i is participating factor.

The reactive power (Q_i) equation remains similar to the single slack bus model since it does not depend on the selected participation factor and is given by:

$$Q_i = - \sum_{k=1}^n |V_i| |V_k| |Y_{ik}| \sin(\theta_{ik} + \delta_k - \delta_i) \tag{2}$$

The ordinary NR matrix thus changes as shown below.

$$\begin{bmatrix} \Delta P_1 \\ \vdots \\ \Delta P_n \\ \Delta Q_1 \\ \vdots \\ \Delta Q_{n-m} \end{bmatrix} = \begin{bmatrix} \left(\frac{\partial P_1}{\partial \delta_1}\right) & \dots & \left(\frac{\partial P_1}{\partial \delta_n}\right) \\ \vdots & \ddots & \vdots \\ \left(\frac{\partial P_n}{\partial \delta_1}\right) & \dots & \left(\frac{\partial P_n}{\partial \delta_n}\right) \\ \left(\frac{\partial Q_1}{\partial \delta_1}\right) & \dots & \left(\frac{\partial Q_1}{\partial \delta_n}\right) \\ \vdots & \ddots & \vdots \\ \left(\frac{\partial Q_{n-m}}{\partial \delta_1}\right) & \dots & \left(\frac{\partial Q_{n-m}}{\partial \delta_n}\right) \end{bmatrix} \begin{bmatrix} \left(\frac{\partial P_1}{\partial |V_1|}\right) & \dots & \left(\frac{\partial P_1}{\partial |V_{n-m}|}\right) & K_i \\ \vdots & \ddots & \vdots & \vdots \\ \left(\frac{\partial P_n}{\partial |V_1|}\right) & \dots & \left(\frac{\partial P_n}{\partial |V_{n-m}|}\right) & K_n \\ \left(\frac{\partial Q_1}{\partial |V_1|}\right) & \dots & \left(\frac{\partial Q_1}{\partial |V_{n-m}|}\right) & \frac{\partial Q_1}{\partial P_{Loss}} \\ \vdots & \ddots & \vdots & \vdots \\ \left(\frac{\partial Q_{n-m}}{\partial |V_1|}\right) & \dots & \left(\frac{\partial Q_{n-m}}{\partial |V_{n-m}|}\right) & \frac{\partial Q_1}{\partial P_{Loss}} \end{bmatrix} \begin{bmatrix} \Delta \delta_1 \\ \vdots \\ \Delta \delta_n \\ \Delta |V_1| \\ \vdots \\ \Delta |V_{n-m}| \\ \Delta P_{Loss} \end{bmatrix} \tag{3}$$

Since the participation factor selected depends only on real powers, some terms in the extended Jacobian matrix above are removed.

For real power in the generator buses, $\frac{\partial P_i}{\partial P_{Loss}} = K_i$, which represents our participation factors. For the load buses, $\frac{\partial P_i}{\partial P_{Loss}} = 0$. The reactive powers are not included in the participation factors. The resulting extended Jacobian matrix is thus reduced as shown below.

$$\begin{bmatrix} \Delta P_1 \\ \vdots \\ \Delta P_n \\ \Delta Q_1 \\ \vdots \\ \Delta Q_{n-m} \end{bmatrix} = \begin{bmatrix} \left(\frac{\partial P_1}{\partial \delta_1}\right) & \dots & \left(\frac{\partial P_1}{\partial \delta_n}\right) \\ \vdots & \ddots & \vdots \\ \left(\frac{\partial P_n}{\partial \delta_1}\right) & \dots & \left(\frac{\partial P_n}{\partial \delta_n}\right) \\ \left(\frac{\partial Q_1}{\partial \delta_1}\right) & \dots & \left(\frac{\partial Q_1}{\partial \delta_n}\right) \\ \vdots & \ddots & \vdots \\ \left(\frac{\partial Q_{n-m}}{\partial \delta_1}\right) & \dots & \left(\frac{\partial Q_{n-m}}{\partial \delta_n}\right) \end{bmatrix} \begin{bmatrix} \left(\frac{\partial P_1}{\partial |V_1|}\right) & \dots & \left(\frac{\partial P_1}{\partial |V_{n-m}|}\right) & K_i \\ \vdots & \ddots & \vdots & \vdots \\ \left(\frac{\partial P_n}{\partial |V_1|}\right) & \dots & \left(\frac{\partial P_n}{\partial |V_{n-m}|}\right) & 0 \\ \left(\frac{\partial Q_1}{\partial |V_1|}\right) & \dots & \left(\frac{\partial Q_1}{\partial |V_{n-m}|}\right) & 0 \\ \vdots & \ddots & \vdots & \vdots \\ \left(\frac{\partial Q_{n-m}}{\partial |V_1|}\right) & \dots & \left(\frac{\partial Q_{n-m}}{\partial |V_{n-m}|}\right) & 0 \end{bmatrix} \begin{bmatrix} \Delta \delta_1 \\ \vdots \\ \Delta \delta_n \\ \Delta |V_1| \\ \vdots \\ \Delta |V_{n-m}| \\ \Delta P_{Loss} \end{bmatrix} \tag{4}$$

2.2 Formulation of Fuel Cost Functions

For thermal generator, it is required to minimize the fuel cost with real power output. This can be done below.

The fuel cost function of each fossil fuel fired generator is expressed as a quadratic function. The total fuel cost in terms of real power output can be expressed as:

$$C(P_{gi}) = \sum_{i=1}^{NG} (a_i P_{gi}^2 + b_i P_{gi} + c_i) \tag{5}$$

Where a_i , b_i and c_i are the fuel cost coefficients of i th unit, NG is the number of generators, and P_{gi} is generator active or real power.

The minimization of fuel cost with reactive power output can also be done. Reactive power production cost is highly dependent on real power output. If a generator produces its maximum active power (P_{max}) then no reactive power is produced. Therefore apparent power equals P_{max} , and reactive power production by a generation will result in reduction of its active power production.

To generator reactive power Q_{gi} by a generator I , it is required to reduce its active power to P_{gi} . Therefore, at the different values of Q_{gi} with respect to P_{gi} , the quadratic cost expression for reactive power is calculated by fitting a curve into a quadratic polynomial. The fuel cost in term of reactive power output can be expressed as:

$$C(Q_{gi}) = \sum_{i=1}^{NG} (a_{gi} Q_{gi}^2 + b_{gi} + c_{gi}) \quad (6)$$

Where a_{gi} , b_{gi} , c_{gi} are reactive power cost coefficients, calculated using a curve fitting, and NG is number of generators.

Furthermore, the operating cost function of the wind farm can be obtained. According to [4], the linear cost function assumed for the wind farm is given as follows:

$$C_{wi}(W_i) = d_i \cdot W_i \quad (7)$$

Where d_i is direct cost coefficient of i th wind farm, and W_i is actual wind power.

For cost junction due to the over-generation, the penalty cost caused by not using all the available wind power is related to the difference between the available wind power and the actual wind power used. The mathematical model is written as follows [4].

$$C_{pwi}(W_{iav} - W_i) = K_{pi}(W_{iav} - W_i) = K_{pi}\{(W - W_i)f_w(W)\} \quad (8)$$

Where K_{pi} is penalty cost coefficient for over generation of i th wind farm, $f_w(w)$ is probability density function (PDF) of wind power output, and W_{iav} is available wind power

For cost function due to the under generation, the cost function of i th wind farm for calling the reservists cover i th wind farm due to under-generation is written as follows [4]

$$C_{rwi}(W_i - W_{iav}) = K_{ri}(W_i - W_{iav}) = K_{ri}\{(W - W_i) f_w(W)\} \quad (9)$$

Where K_{ri} is reserve cost coefficient for under generation of i th wind farm.

Therefore, the overall cost functions for the wind farm is:

$$C_{wi}(W_i) + C_{pwi}(W_{iav} - W_i) + C_{rwi}(W_i - W_{iav}) \quad (10)$$

2.2.1 Constraints

The total real power generation by each generating unit must balance the predicted real power demand plus the real power losses

$$\sum_{i=1}^{NG} P_{gi} - \sum_{i=1}^{NB} P_{oi} - P_L = 0 \quad (11)$$

Where P_{oi} is active power demand on the i th bus, NB is number of buses, and P_L is real power losses.

Similarly, for reactive power

$$\sum_{i=1}^{NG} Q_{gi} - \sum_{i=1}^{NB} Q_{oi} - Q_L = 0 \quad (12)$$

Where Q_{oi} is reactive power demand on the i th bus, NB is number of buses, NG is number of generators, and Q_L is reactive losses.

Active and reactive power operating limit (generation capacity limits) is given by

$$P_{gi}^{min} \leq P_{gi} \leq P_{gi}^{max} \quad (i=1, 2 \dots NG) \quad (13)$$

Where P_{gi}^{min} and P_{gi}^{max} are the minimum and maximum limits for active power generation by i th unit.

The power balance constraints to be satisfied for thermal and wind energy are [5]:

Real power balance constraints

$$\sum_{i=1}^{NG} P_{gi} + \sum_{i=1}^{NW} P_{wi} - \sum_{i=1}^{NB} P_{Di} - \sum P_L = 0 \quad (14)$$

And

Reactive power balance constraints

$$\sum_{i=1}^{NG} Q_{gi} + \sum_{i=1}^{NW} Q_{wi} - \sum_{i=1}^{NB} Q_{Di} - \sum Q_L = 0 \quad (15)$$

Where P_{Di} and Q_{Di} are active and reactive power drawn, while, P_{wi} , and Q_{wi} are the active and reactive wind power.

2.3 Algorithm

This section discusses the solution algorithm for real and reactive power participation factors. The real power participation factors developed in [3] for the general distributed generator and the reactive power distributed slack model for the NR method is developed in [6] to distribute the reactive slack. The NR method is selected for the distributed slack bus model because, as compared to the Gauss Siedel method (GS), NR has the following merits:

1. Its rate of convergence is fast and therefore requires less number of iterations to obtain the solution.
2. It is independent of the number of buses of the system hence it can be applied on large practical systems.
3. The convergence of the method is not affected by the selection of the slack bus; hence there is freedom of distributing the slack bus.
4. It is more accurate and reliable when used for large systems.

However, the feature that automatically disqualifies the GS and Fast Decoupled method as a method to be used in the power flow analysis of the DSB model is the fact that all the other methods are sensitive to the position of the slack bus. NR method is not sensitive to the position of the slack bus and is therefore an ideal choice for power flow for the DSB model

2.3.1 Distributed slack bus algorithm based on real power participation factors

The distributed slack bus selected based on a real power generator output participation factors is implemented using a NR solver. The selected algorithm is illustrated below.

Step 1: Read system data and formulate Y_{bus}

Step 2: Initialize bus voltage magnitudes $|V_i|$, phase angles δ and set initial $P_{Loss} = 0$

Step 3: Set iteration counter $K = 0$ and convergence criteria ϵ

Step 4: Set initial values of P_{gi} and determine initial participation factor K_i^0

Step 5: Compute $P_i^{(k)}$ and $Q_i^{(k)}$ for system buses using the equations:

$$P_i = \sum_{k=1}^n |V_i| |V_k| |Y_{ik}| \cos(\theta_{ik} + \delta_k - \delta_i) + K_i * P_{Loss}$$

$$Q_i = - \sum_{k=1}^n |V_i| |V_k| |Y_{ik}| \sin(\theta_{ik} + \delta_k - \delta_i)$$

Step 6: Compute residuals $\Delta P_i^{(k)}$ and $\Delta Q_i^{(k)}$

Step 7: Compute largest of absolute residues of P_i and Q_i between two successive iterations:

- If residue $< \epsilon$: STOP

- If not, Compute elements of the extended Jacobian (Je) where $Je = \frac{dF}{dx}$ for each iteration.

Step 8: Solve for $Je^{(k)} \Delta X^{(k)} = -F^{(k)}$

Step 9: Update values of V_i , δ_i and P_{Loss} for the next iteration i.e. $x^{(k+1)} = x^{(k)} + \Delta X^{(k)}$

Step 10: Let $K = K+1$

Step 11: Check real and reactive limits of the participating generators. If it violates the limits, we change it into a constant PQ injection, increment the counter and go to step 4.

Step 12: If generator limits are not violated, we then calculate the participation factor K_i and go to step 5.

2.3.2 Distributed slack bus algorithm based on reactive power participation factors

The distributed slack bus selected based on a real power generator output participation factors is implemented using a NR solver by as shown above. This paper develops a distributed slack bus algorithm based on reactive power participation factors as follows:

Step 1: Read system data and formulate Y_{bus}

Step 2: Initialize bus voltage magnitudes $|V_i|$, phase angles δ and set initial $Q_{Loss} = 0$

Step 3: Set iteration counter $K = 0$ and convergence criteria ϵ

Step 4: Set initial values of Q_{gi} and determine initial reactive power participation factor K_i^0

Step 5: Compute $P_i^{(k)}$ and $Q_i^{(k)}$ for system buses using the equations:

$$P_i = \sum_{k=1}^n |V_i| |V_k| |Y_{ik}| \cos(\theta_{ik} + \delta_k - \delta_i)$$

$$Q_i = -\sum_{k=1}^n |V_i| |V_k| |Y_{ik}| \sin(\theta_{ik} + \delta_k - \delta_i) + K_t * P_{Loss}$$

Step 6: Compute residuals $\Delta P_i^{(k)}$ and $\Delta Q_i^{(k)}$

Step 7: Compute largest of absolute residues of P_i and Q_i between two successive iterations:

- If residue $< \epsilon$: STOP

- If not, Compute elements of the extended Jacobian (Je) where $Je = \frac{dF}{dx}$

for each iteration

Step 8: Solve for $Je^{(k)} \Delta x^{(k)} = -F^{(k)}$

Step 9: Update values of V_i , δ_i and Q_{Loss} for the next iteration i.e. $x^{(k+1)} = x^{(k)} + \Delta x^{(k)}$

Step 10: Let $K = K+1$

Step 11: Check real and reactive limits of the participating generators. If it violates the limits, we change it into a constant PQ injection, increment the counter and go to step 4.

Step 12: If generator limits are not violated, we then calculate the participation factor K_t and go to step 5.

2.4 Flow Charts

Fig.1 shows Flow chart of the distributed slack bus algorithm

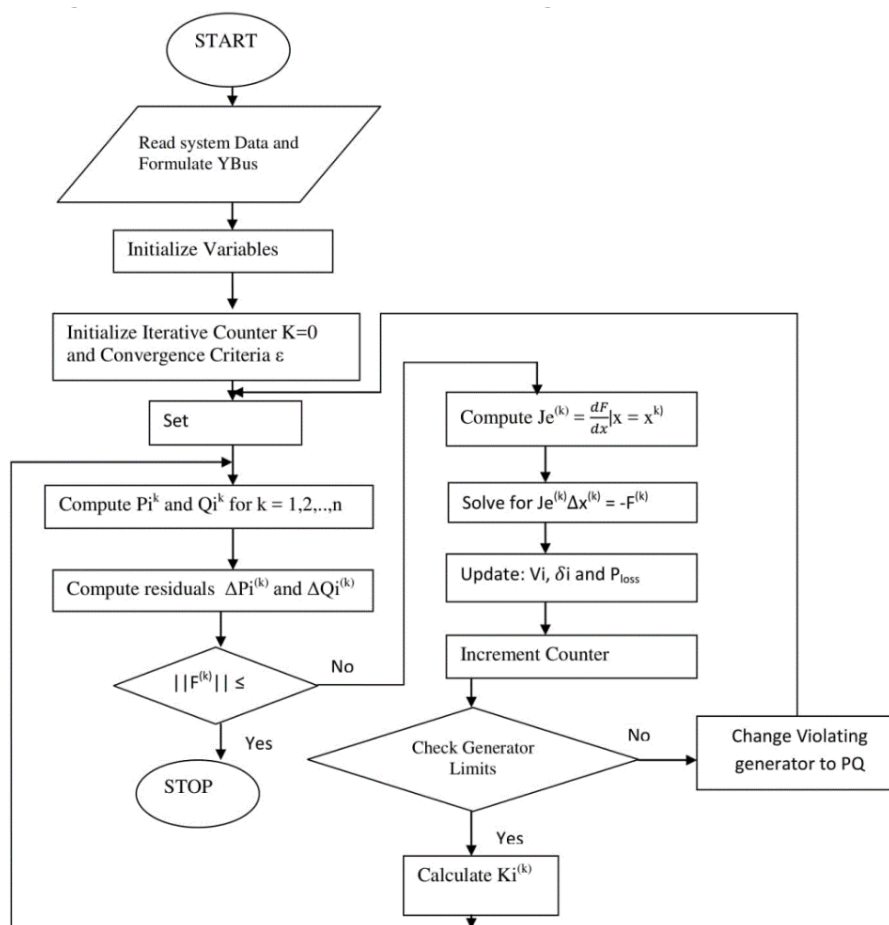


Fig.1 Flow chart of the distributed slack bus

3. Results and analysis

3.1 Case study

3.1.1 IEEE 14 Bus Test Network

A one line diagram for the test network is shown Fig.2.

For the distributed slack bus, bus 1 is considered as a PV bus. Table 1 shows bus data for IEEE 14 bus test network, while Table 2 and Table 3 show line data for IEEE 14 bus test network, and cost coefficients for IEEE 14 bus respectively.

Table 1 Bus data for IEEE 14 bus test network

Bus	Type	Specified voltage	Angle	Real Power Gen (MW)	Reactive Power Gen (MVAR)	Load P1 (MW)	Load Q1 (MVAR)	Qmin	Qmax
1	SLACK	1.06	0	232.4	-16.9	0	0	0	0
2	PV	1.045	0	40	42.4	21.7	12.7	-40	50
3	PV	1.01	0	0	23.4	94.2	19.0	0	0
4	PQ	1.0	0	0	0	47.8	-3.9	0	0
5	PQ	1.0	0	0	0	7.6	1.6	0	0
6	PV	1.07	0	0	12.2	11.2	7.5	-6	24
7	PQ	1.0	0	0	0	0	0	0	0
8	PV	1.09	0	0	17.4	0	0	-6	24
9	PQ	1.0	0	0	0	29.5	16.6	0	0
10	PQ	1.0	0	0	0	9	5.8	0	0
11	PQ	1.0	0	0	0	3.5	1.8	0	0
12	PQ	1.0	0	0	0	6.1	1.6	0	0
13	PQ	1.0	0	0	0	13.5	5.8	0	0
14	PQ	1.0	0	0	0	14.9	5.0	0	0

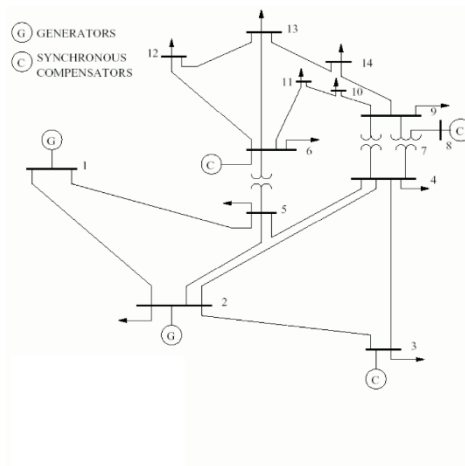


Fig.2 IEEE 14 bus test network

Table 2 Line data for IEEE 14 bus test network

From Bus	To Bus	Resistance (p.u)	Reactance (p.u)	Half-line susceptance(B/2)	Transformer tap Settings
1	2	0.01938	0.05917	0.0264	1
2	3	0.04699	0.19797	0.0219	1
2	4	0.05811	0.17632	0.0187	1
1	5	0.05403	0.22304	0.0246	1
2	5	0.05695	0.17388	0.01730	1
3	4	0.06701	0.17103	0.0064	1
4	5	0.01335	0.04211	0	1
5	6	0	0.25202	0	0.932
4	7	0	0.20912	0	0.978
7	8	0	0.17615	0	1
4	9	0	0.55618	0	0.969
7	9	0	0.11001	0	1
9	10	0.03181	0.0845	0	1
6	11	0.09498	0.19890	0	1
6	12	0.12291	0.25581	0	1
6	13	0.06615	0.13027	0	1
9	14	0.12711	0.27038	0	1
10	11	0.08205	0.19207	0	1
12	13	0.22092	0.19988	0	1
13	14	0.17093	0.34802	0	1

Table 3 Cost coefficients for IEEE 14 bus

Gen No.	a_i (\$/MWhr) ²	b_i (\$/MWhr)	C_i \$/hr
1	0.0430293	20	100
2	0.25	20	70
3	0.01	40	100
4	0.01	40	70
5	0.01	40	40

3.2 Results and validation

3.2.1 IEEE 14 bus results

3.2.1.1 Ordinary NR using single slack bus

Table 4 shows IEEE 14 bus output data with single slack bus, while Table 5 shows IEEE 14 bus line flows and losses with single slack bus.

Table 4 IEEE 14 bus output data with single slack bus

Bus No.	V (pu)	Angle	P _G	Q _G	P _L	Q _L	P _I	Q _I
1	1.0600	0.0000	232.593	-15.233	0.000	0.000	232.593	-15.233
2	1.0450	-4.989	40.000	47.928	21.700	12.700	18.300	35.228
3	1.0100	-12.7487	0.000	27.758	94.200	19.000	-94.200	8.758
4	1.0133	-10.2429	0.000	0.000	47.800	-3.900	-47.800	3.900
5	1.0166	-8.7606	0.000	0.000	7.600	1.600	-7.600	-1.600
6	1.0700	-14.447	0.000	0.000	11.200	7.500	-11.200	15.526
7	1.0457	-13.2375	0.000	23.026	0.000	0.000	0.000	0.000
8	1.0800	-13.2375	0.000	0.000	0.000	0.000	0.000	21.030
9	1.0306	-14.8207	0.000	21.030	29.500	16.600	-29.500	-16.600
10	1.0299	-15.0365	0.000	0.000	9.000	5.800	-9.000	-5.800
11	1.0461	-14.8584	0.000	0.000	3.500	1.800	-3.500	-1.800
12	1.0533	-15.2974	0.000	0.000	6.100	1.600	-6.100	-1.600
13	1.0466	-14.2814	0.000	0.000	13.500	5.800	-13.500	-5.800
14	1.0193	-16.0721	0.000	0.000	14.900	5.000	-14.900	-5.000
TOTAL			272.593	104.509	259.000	73.500	13.593	31.009

Generation cost:

SSB thermal cost: 4814.131 \$/Hr

SSB overall cost: 4781.009 \$/Hr

Convergence achieved after: 7 iterations

Table 5 IEEE 14 bus line flows and losses with single slack bus

From-To	P(MW)	Q(Mvar)	From-To	P(MW)	Q(Mvar)	Loss (MW)	Loss(Mvars)
1-2	157.080	-17.484	2-1	-152.772	30.369	4.309	13.155
1-5	75.513	7.981	5-1	72.740	3.464	2.773	11.455
2-3	73.396	5.936	3-2	71.063	3.894	2.333	9.830
2-4	55.943	2.935	4-2	54.273	2.132	1.670	5.067
2-5	41.733	4.738	5-2	40.813	-1.929	0.920	2.890
3-4	-23.137	7.752	4-3	23.528	-6.753	0.391	0.998
4-5	-59.585	11.574	5-4	60.064	-10.063	0.479	1.511
4-7	27.066	-15.396	7-4	-27.066	17.372	0.000	1.932
4-9	15.464	-2.640	9-4	15.464	3.932	0.000	1.292
5-6	45.889	-20.843	6-5	-45.889	26.617	0.000	5.774
6-11	8.287	8.898	11-6	-8.165	-8.641	0.123	0.257
6-12	8.064	3.176	12-6	-7.9485	-3.008	0.081	0.168
6-13	18.337	9.981	13-6	-18.085	-9.485	0.252	0.496
7-8	0.000	-20.362	8-7	0.000	21.030	0.000	0.668
7-9	27.066	14.798	9-7	-27.066	-13.840	0.000	0.957
9-10	4.393	-0.904	10-9	-4.387	0.920	0.006	0.016
9-14	8.637	0.321	14-9	-8.547	-0.131	0.089	0.190
10-11	-4.613	-6.720	11-10	4.665	6.841	0.051	0.120
12-13	1.884	1.408	13-12	-1.873	-1.398	0.011	0.010
13-14	6.458	5.083	14-13	-6.353	-4.869	0.105	0.215
TOTAL LOSS						13.593	56.910

3.2.1.2 IEEE 14 bus distributed slack bus model

Table 6 shows bus output data with distributed slack bus using real power PF. Table 7 shows IEEE 14 bus line flows and losses with distributed slack bus using real power PF, while, Table 8 and Table 9 show IEEE 14 bus output data with distributed slack bus using reactive power PF, and IEEE 14 bus line flows and losses with distributed slack bus for reactive power PF respectively.

Table 6 IEEE 14 bus output data with distributed slack bus using real power PF

Bus No.	V (pu)	Angle	P _G	Q _G	P _L	Q _L	P _I	Q _I
1	1.0700	11.8713	232.408	6.325	0.000	0.000	232.408	6.325
2	1.0450	7.1139	40.001	27.802	21.700	12.700	18.301	15.102
3	1.0100	-0.6377	0.000	27.037	94.200	19.000	-94.200	8.037
4	1.0144	1.8474	0.000	0.000	47.800	-3.900	-47.800	3.900
5	1.0186	3.3143	0.000	0.000	7.600	1.600	-7.600	-1.600
6	1.0700	-2.3537	0.000	21.944	11.200	7.500	-11.200	14.444
7	1.0462	-1.1461	0.000	0.000	0.000	0.000	0.000	0.000
8	1.0800	-1.1461	0.000	20.695	0.000	0.000	0.000	20.695
9	1.0311	-2.7297	0.000	0.000	29.250	16.600	-29.500	-16.600
10	1.0304	-2.9452	0.000	0.000	9.000	5.800	-9.000	-5.800
11	1.0464	-2.7663	0.000	0.000	3.500	1.800	-3.500	-1.800
12	1.0533	-3.2039	0.000	0.000	6.100	1.600	-6.100	-1.600
13	1.0467	-3.2385	0.000	0.000	13.500	5.800	-13.500	-5.800
14	1.0196	-3.9797	0.000	0.000	14.900	5.000	-14.900	-5.000
TOTAL			272.409	103.803	259.000	73.500	13.409	30.303

Table 7 IEEE 14 bus line flows and losses with distributed slack bus using real power PF

From-To	P(MW)	P(MW)	From-To	P(MW)	P(MW)	Loss (MW)	Loss(Mvars)
1~2	156.840	0.349	2~1	-152.677	12.364	4.164	12.713
2~3	75.567	11.815	3~2	-72.807	-0.419	2.761	11.397
2~4	73.320	5.944	4~2	-70.991	3.866	2.328	9.810
1~5	55.924	2.243	5~1	-54.257	2.815	1.667	5.058
2~5	41.735	3.572	5~2	-40.820	-0.778	0.915	2.794
3~4	-23.209	7.058	4~3	23.595	-6.071	0.387	0.987
4~5	-59.725	9.739	5~4	60.200	-8.241	0.475	1.499
5~6	27.100	-15.087	6~5	-27.100	16.999	0.000	1.912
4~7	15.487	-2.515	7~4	-15.487	3.804	0.000	1.289
7~8	45.827	-20.042	8~7	-45.827	25.706	0.000	5.664
4~9	8.253	8.793	9~4	-8.132	-8.541	0.121	0.253
7~9	8.057	3.163	9~7	-7.976	-2.996	0.080	0.167
9~10	18.317	9.927	10~9	-18.066	-9.433	0.251	0.494
6~11	0.000	-20.049	11~6	0.000	20.695	0.000	0.647
6~12	27.100	14.825	12~6	-27.100	-13.866	0.000	0.959
6~13	4.424	-0.807	13~6	-4.418	0.823	0.006	0.016
9~14	8.662	0.384	14~9	-8.572	-0.192	0.090	0.191
10~11	-4.582	-6.623	11~10	4.632	6.741	0.050	0.117
12~13	1.876	1.396	13~12	-1.865	-1.386	0.011	0.010
13~14	6.432	5.019	14~13	-6.328	-4.808	0.104	0.211
TOTAL LOSS					13.409	56.187	

Generation cost:

DSB thermal cost: 4801.906

DSB overall cost: 4768.870

Convergence achieved after: 6 iterations

Table 8 IEEE 14 bus output data with distributed slack bus using reactive power PF

Bus No.	V (pu)	Angle	P _G	Q _G	P _L	Q _L	P _I	Q _I
1	1.0500	12.0665	223.861	-35.774	0.000	0.000	223.861	-35.774
2	1.0450	7.0834	46.150	57.193	21.700	12.700	24.450	44.493
3	1.0200	-0.6686	2.287	37.215	94.200	19.000	-91.913	18.215
4	1.0142	1.8161	-1.790	-5.224	47.800	-3.900	-49.590	-1.324
5	1.0172	3.3072	2.114	-0.211	7.600	1.600	-5.486	-1.811
6	1.0800	-2.3425	7.030	40.454	11.200	7.500	-4.170	32.954
7	1.0503	-1.1766	-0.000	-5.963	0.000	0.000	-0.000	-5.963
8	1.1000	-1.1738	0.032	31.006	0.000	0.000	0.032	31.006
9	1.0337	-2.7573	-0.000	0.000	29.500	16.600	-29.500	-16.600
10	1.0326	-2.9662	-0.000	0.000	9.000	5.800	-9.000	-5.800
11	1.0475	-2.7727	-2.080	-4.273	3.500	1.800	-5.580	-6.073
12	1.0535	-3.1932	-1.657	-3.322	6.100	1.600	-7.757	-4.922
13	1.0471	-3.2329	-3.344	-6.339	13.500	5.800	-16.844	-12.139
14	1.0213	-3.9896	-0.000	0.000	14.900	5.000	-14.900	-5.000
TOTAL			272.603	104.762	259.000	73.500	13.603	31.262

Table 9 IEEE 14 bus line flows and losses with distributed slack bus for reactive power PF

From-To	P(MW)	Q(Mvars)	From-To	P(MW)	Q(Mvars)	Loss (MW)	Loss(Mvars)
1~2	150.170	-33.304	2~1	-146.011	46.002	4.159	12.698
2~3	73.691	3.152	3~2	-71.025	7.853	2.666	11.006
2~4	72.822	0.832	4~2	-70.540	8.783	2.282	9.615
1~5	55.951	2.328	5~1	-54.282	2.736	1.669	5.063
2~5	41.689	4.351	5~2	-40.772	-1.554	0.916	2.797
3~4	-21.374	12.377	4~3	21.767	-11.374	0.393	1.003
4~5	-59.781	12.541	5~4	60.265	-11.014	0.484	1.527
5~6	27.194	-17.195	6~5	-27.194	19.253	0.000	2.058
4~7	15.512	-3.045	7~4	-15.512	4.354	-0.000	1.309
7~8	46.047	-24.905	8~7	-46.047	31.125	0.000	6.221
4~9	10.349	12.729	9~4	-10.130	-12.270	0.219	0.459
7~9	9.751	6.551	9~7	-9.606	-6.248	0.145	0.303
9~10	21.776	16.317	10~9	-21.356	-15.490	0.420	0.827
6~11	-0.032	-29.606	11~6	0.032	31.006	0.000	1.400
6~12	27.226	16.257	12~6	-27.226	-15.254	-0.000	1.003
6~13	4.501	-0.278	13~6	-4.495	0.294	0.006	0.016
9~14	8.737	0.724	14~9	-8.646	-0.529	0.091	0.194
10~11	-4.505	-6.094	11~10	4.550	6.197	0.044	0.103
12~13	1.849	1.327	13~12	-1.839	-1.317	0.010	0.009
13~14	6.351	4.668	14~13	-6.254	-4.471	0.097	0.197
TOTAL LOSS						13.603	57.809

Generation cost:

DSB reactive with RE cost: 757.623 \$/Hr

DSB reactive thermal cost: 834.150 \$/Hr

Convergence achieved after: 4 iterations

Therefore the total cost is:

DSB with RE using combined PF (Thermal): $(4801.906*0.8) + (834.150*0.2) = 4008.3548$ \$/Hr

DSB with RE using combined PF (With RE): $(4768.870*0.8) + (757.623*0.2) = 3966.6206$ \$/Hr

3.3 Analysis and discussion

Table 10 and Table 11 show comparison of generated real power, and comparison of generation costs, respectively.

Table 10 Comparison of generated real power

		Single Slack Bus Model	Distributed Slack Bus using Real Power PF	Distributed Slack Bus using Reactive Power PF
Generation:	Plant 1	232.593 MW	232.408 MW	223.861 MW
	Plant 2	40.000 MW	40.001 MW	46.150 MW
Total System Losses		13.593 MW	13.409 MW	13.603 MW

Table 11 Comparison of generation costs

	Single Slack Bus Model	Distributed Slack Bus Model With Real Power PF	Distributed Slack Bus Model With Combined PF
Generation Cost for Thermal Generators (\$/Hr)	4814.131	4801.906	4008.3548
Generation Cost for Thermal & RE Generators (\$/Hr)	4781.009	4768.870	3966.6206

Fig.3 and Fig.4 show the voltage profile comparison, and voltage angle comparison respectively.

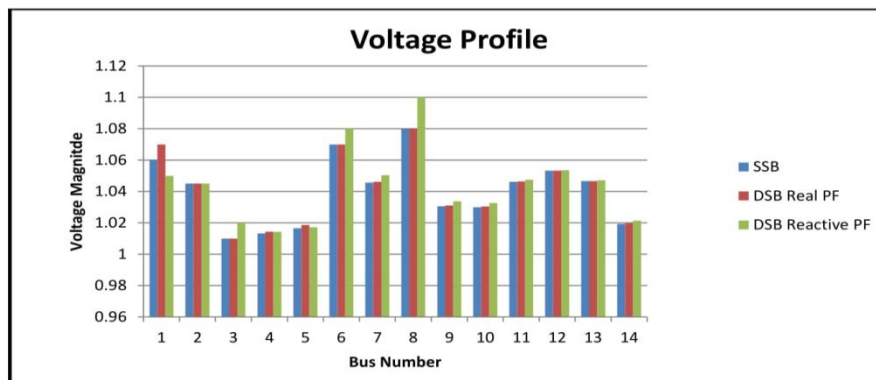


Fig.3 Voltage profile comparison

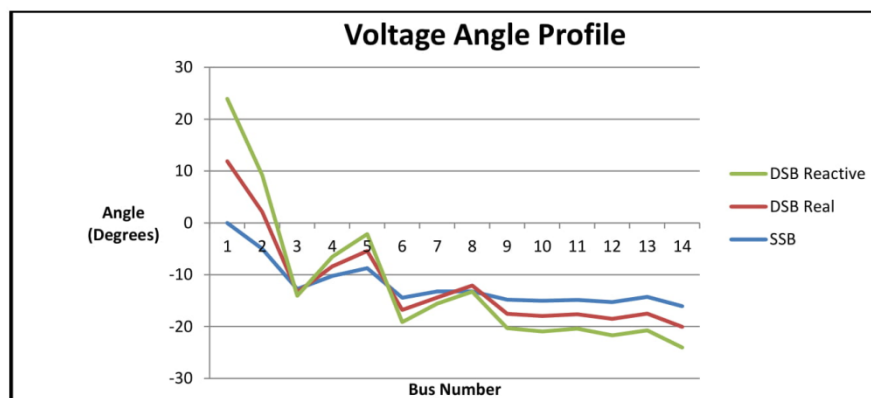


Fig.4 Voltage angle comparison

From Fig.3, it is observed that the voltage magnitudes between buses are relatively similar. Voltage angles vary significantly in the two models as shown in Fig.4. In the SSB model, bus 1 was taken as the reference bus with a phase angle of 0. With the DSB models, the DSB distributes system mismatches to all PV buses in the system through participation factors resulting in a change in phase angles. Power losses reduce by 0.184 MW in the DSB model using real power participation factors compared to the SSB. However, the DSB using reactive power participation factors does not improve on the losses, this is because reactive power represents the power absorbed by the system. The generator real power outputs with a DSB are slightly less than the real power outputs with a SSB as illustrated in Table 10. This results in a lower generation cost in the DSB model as demonstrated in

Table 11. The incorporation of renewable energy reduces the cost of generation in both the SSB and DSB as demonstrated in Table 11.

4 Conclusion

Slack bus modeling for distribution power flow analysis has been studied and investigated. Firstly, the distribution power with a DSB model has been studied. Secondly, scalar participation factors to distribute uncertain real and reactive power system losses have been used for three phase power flow calculations. Finally, renewable energy sources including wind and solar generators have been incorporated in the system as distributed generators and the cost of generation has been compared to that of a system without renewable energy. The DSB provided a realistic approach to analyzing a power system as compared to the SSB and emerged as a more realistic technique to be employed in deregulated distributed generation systems involving renewable energy. The DSB has an effect of distributing the system losses thereby allowing dispersed generators to adjust their outputs appropriately to meet the load and loss requirements of the network. This is achieved through application of participation factors combined participation factors based on the generation capacity. The algorithm developed has been found to be robust and can be implemented in larger systems. The developed DSB can be applied in; capacitor placement and sizing, network reconfiguration, distributed system expansion and service restoration.

References

1. O. Billy, "Distributed slack bus for economic dispatch of renewable energy", Graduation Project, University of Nairobi, Kenya, 2015.
2. A. Mohapatra, "Distributed slack bus algorithm for economic load dispatch", B. Tech Thesis, NIT Rourkela, 2012.
3. T. Shiqiong, M. Kleinberg, and K. Miu, "A distributed slack bus model and its impact on distribution system application techniques", IEEE International Symposium on Circuits and Systems, Japan, 2005.
4. R. Jabr, and B.C. Pal, "Intermittent wind generation in optimal power flow dispatching", IET Generation, Transmission and Distribution, Vol. 3, No.1, PP.66 -74, 2009.
5. M. Amita, V. Prasad, and S. Rangnekar, "Economic dispatch using particle swarm optimization: A review", Renewable and Sustainable Energy Reviews, Vol.13, Issue 8, PP.2134-2141, 2009.
6. P. Musau, and N. Odero, "Distributed slack bus model for a wind-based distributed generation using combined participation factors" International Journal of Emerging Technology and Advanced Engineering, Vol.2, Issue 10 PP.459-469, 2012.

Надійшла 20.05.2019

Received 20.05.2019

УДК 621.3.011.74.005

В.В. Михайленко, канд. техн. наук, доцент, ORCID 0000-0002-0973-4612

В.А. Святненко, старший викладач, ORCID 0000-0002-0518-1045

Ю.М. Чуняк, асистент, ORCID 0000-0002-4506-912X

О.С. Чарняк, студентка

Національний технічний університет України «Київський політехнічний інститут імені Ігоря Сікорського»

ДОСЛІДЖЕННЯ ЕЛЕКТРОМАГНІТНИХ ПРОЦЕСІВ У ПЕРЕТВОРЮВАЧІ З ОДИНАДЦЯТИЗОННИМ РЕГУЛЮВАННЯМ НАПРУГИ

Метою роботи є розробка математичної моделі напівпровідникового перетворювача з високочастотним широтно-імпульсним перетворенням параметрів електричної енергії з використанням пакету MATHCAD.

У цій статті проведено аналіз електромагнітних процесів в електричних колах напівпровідниковими з комутаторами. Створено математичну модель для аналізу електромагнітних процесів в напівпровідникових перетворювачах з широтно-імпульсним регулюванням вихідної напруги. Наведено графіки, що відображають електромагнітні процеси у електричних колах. Стаття присвячена розвитку метода багатопараметричних функцій шляхом розробки нових математичних моделей та визначення функцій і алгоритмічних рівнянь для аналізу за підсистемними складовими електромагнітних процесів у розгодуваних електричних колах з напівпровідниковими комутаторами і ланками з синусоїдальними, постійними і імпульсними напругами. Напівпровідникові комутатори можуть виконувати високочастотне

© В.В. Михайленко, В.А. Святненко, Ю.М. Чуняк, О.С. Чарняк, 2019